

Joint Flow And Feature Refinement Using Attention For Video Restoration

Ranjith Merugu²

ranjith.merugu@stonybrook.edu

Mohammad Sameer Suhail*¹

mo.suhail@samsung.com

Akshay P Sarashetti*¹

akshay.p@samsung.com

Venkata Bharath Reddy Reddem*¹

r.reddy@samsung.com

Pankaj Kumar Bajpai¹

pankaj.b@samsung.com

Amit Satish Unde¹

amit.unde@samsung.com

Abstract

Recent advancements in video restoration have focused on recovering high-quality video frames from low-quality inputs. Compared with static images, the performance of video restoration significantly depends on efficient exploitation of temporal correlations among successive video frames. The numerous techniques make use of temporal information via flow-based strategies or recurrent architectures. However, these methods often encounter difficulties in preserving temporal consistency as they utilize degraded input video frames. To resolve this issue, we propose a novel video restoration framework named Joint Flow and Feature Refinement using Attention (JFFRA). The proposed JFFRA is based on key philosophy of iteratively enhancing data through the synergistic collaboration of flow (alignment) and restoration. By leveraging previously enhanced features to refine flow and vice versa, JFFRA enables efficient feature enhancement using temporal information. This interplay between flow and restoration is executed at multiple scales, reducing the dependence on precise flow estimation. Moreover, we incorporate an occlusion-aware temporal loss function to enhance the network's capability in eliminating flickering artifacts. Comprehensive experiments validate the versatility of JFFRA across various restoration tasks such as denoising, deblurring, and super-resolution. Our method demonstrates a remarkable performance improvement of up to 1.62 dB compared to state-of-the-art approaches.

1. Introduction

With advances in smart phones cameras and its widespread use, user-generated content in the form of images/videos is exponentially growing. However, despite significant progress in camera sensor technology, videos captured us-

ing mobile cameras suffer from degradation in perceptual quality due to the presence of noise, blur and compression artifacts [1, 17]. The artifacts in captured videos are complex and stochastic in nature. It causes severe degradation, especially in unconstrained scenarios such as data acquisition in low-light environment, low-cost mobile devices and unwanted camera movement. Removing degradation is challenging, as these inverse problems are ill-posed [27, 30]. Therefore, video restoration [17, 19, 21–23] which is the process of bringing videos back to life by enhancing its quality is an important problem in the field of computer vision.

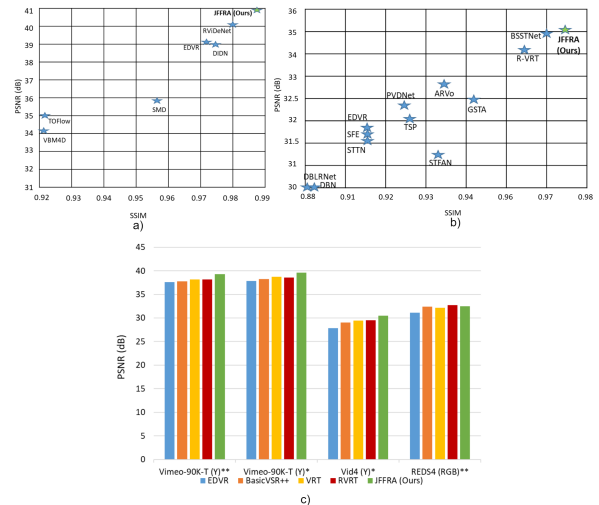


Figure 1. The proposed JFFRA framework achieves the state-of-the-art performance on various video restoration tasks such as a) Video Denoising, b) Video Deblurring, and c) Video Super-resolution.

Video restoration [22, 23] is gaining an attention of research community owing to increased potential of storage and processing power of mobile devices and cloud computing. The key challenges in video restoration can be categorized into two streams as (1) exploiting temporal correlation between adjacent frames and (2) flicker removal. Over the past few years, variety of video restora-

*Equal contribution

¹Samsung R&D Institute India, Bangalore

²Stony Brook University

tion algorithms [17, 23, 41] ranging from classical methods [4, 5, 17, 19, 22, 23, 34, 40, 45] to emerging learning based approaches have been proposed in the literature. After an exhaustive survey, it is noticed that classical methods based on either frame averaging, spatio-temporal patch based processing or non-local-means filtering fail to model inter-frame temporal correlation effectively, resulting in sub-optimal performance. With the emergence of convolutional neural network (CNN), deep-CNN based algorithms for video restoration [14, 23–25] has shown significant improvement in the performance and is the promising research direction.

The CNN-based methods exploit temporal redundancy through implicit or explicit motion modeling. The implicit motion modeling can be achieved through multi-frame processing, recurrent neural network or Long Short-term Memory (LSTM)[33, 56] which holds the potential to model spatio-temporal correlation between adjacent frames. Albeit promising, these methods lacks in fully exploiting the temporal redundancy between adjacent frames and can be prone to error accumulation. This problem of inadequate correlation exploitation can be alleviated through explicit motion modeling using optical flow [12, 36, 39].

The optical flow based restoration algorithms [37, 51] first estimate motion vectors between frames. The temporal alignment across consecutive frames is accomplished through warping of pixels from adjacent frames with respect to a common reference frame. This alignment facilitates the restoration process through the exploitation of temporal coherence. It also ensures that degradation patterns are consistently addressed across the video frames. However, the warping operation can lead to troublesome ghosting problem, which may cause performance degradation. In addition, optical flow based methods also suffer from inevitable and challenging occlusion [46] problem, further damaging performance.

To overcome the drawbacks of optical flow, attention mechanisms [6, 44, 48] have become pivotal, particularly for tasks that require spatial and temporal processing. In this direction, the current state-of-the-art networks such as video restoration transformer (VRT) [23] leverages on mutual and self-attention mechanism to model long-range spatio-temporal dependency. While VRT demonstrated significant performance gains for different video restoration tasks, it has two major limitations. First, its long-range temporal information modeling ability is limited. This can be attributed to the use of window based attention mechanism for implicit motion estimation on image features. Hence, VRT fails to handle large motions efficiently. Second, the implicit motion modeling in feature space is reminiscent of learning un-referenced functions which are difficult to optimize. Therefore, this implicit motion modeling can be more error-prone, particularly while modeling sufficiently moder-

ate motions.

In this paper, we address the problems associated with both implicit and explicit motion modeling through joint refinement of flow and frame features. We propose Joint Flow and Feature Refinement using Attention (JFFRA) network that handles three major problems: (1) it prevents errors in implicit motion modeling by utilizing initial flow computed on the input frames, (2) through iterative flow and feature refinement it continually corrects the explicit motion modeling, and (3) by utilizing a novel occlusion-aware temporal loss function it reduces the misalignment between restored frames, reducing the flickering problem in video restoration tasks.

Our main contributions can be summarized as follows:

1. We propose a novel Joint flow and feature refinement using Attention (JFFRA) module that iteratively refines the flow and frame features in collaborative manner, resulting in continual improvement of motion modeling and restoration.
2. We introduce a novel occlusion-aware temporal loss function that handles the temporal alignment across restored frames and eliminate flickering artifacts.
3. To the best of our knowledge, we are the first to demonstrate that iterative refinement with mutual reinforcement between flow (alignment) and restoration consistently outperforms the end-to-end learning method in terms of restored video frames quality.
4. We validate the effectiveness and generality of proposed JFFRA approach on range of video restoration task such as denoising, superresolution and deblurring, achieving state-of-the-art (SOTA) performance and outperforming the existing methods by up to 1.62 dB on benchmark datasets as shown in Figure 1.

2. Related Work

In this section, we briefly review related work on video restoration and optical flow.

2.1. Video Restoration

Early video-restoration methods leveraged recurrent networks to capture sequential information effectively. Recent advancements have seen improvements such as enhanced grid propagation [29, 55], flow based alignment techniques and deformable convolutions [6, 45, 62]. Some approaches have adopted asymmetric loss functions to optimize network performance, while others have proposed patch-based algorithms [3, 43] that exploit correlations among patches for better restoration. Combining patch-based frameworks [42, 43] with convolution neural networks has also been explored, leading to the development of more sophisticated patch-crafting techniques. Additionally, self-supervised learning techniques have been applied to handle unknown degradation effectively. Blind restora-

tion methods [10, 60] trained on diverse degradations have also emerged. State-of-the-art techniques, including video restoration transformers [8, 23] with parallel frame prediction, have set new benchmarks in the field. However, existing optical-flow-based methods [37, 51] often overlook the impact of degradation on flow estimation, which can result in incorrect feature alignment. While task-oriented flow learning approaches have been proposed, they sometimes fail to refine and compensate for inaccuracies in flow estimation comprehensively.

To address this issue, a novel JFFR block is proposed that aligns features with flow values and refines flow using the corrected features. The alignment of features with the refined flow enhances the quality of video-restoration results.

2.2. Optical Flow

Optical flow estimation is crucial in any video enhancement task. The idea of optical flow was first proposed in Flownet [12], recent advancements show that flow could be used in multiple tasks. Video restoration tasks [23, 25, 38] achieved state-of-the-art results utilizing flow for frame alignment. The flow computed on degraded frames can be corrupted. So, flow correction is necessary for video enhancements [25, 37]. To improve the efficiency of alignment, a novel refinement block is proposed in this paper that refines flow based on intermediate frame features and vice versa, both of which are progressively improvised over the original optical flow and degraded frames respectively. The refined flow is used as offset to guide the network for more coherent temporal alignment in intermediate frame features. These refined frame features are again used to correct the flow.

3. Proposed Methodology

3.1. Overall Framework

Let $I^{LQ} \in \mathbb{R}^{T \times H \times W \times C}$ be a sequence of degraded low-quality frames (LQ) input frames and $I^{HQ} \in \mathbb{R}^{T \times H \times W \times C}$ be a sequence of high-quality ground-truth frames (HQ). T , H , W , C represents frame number, height, width, channel number respectively. We consider $2N + 1$ consecutive frames as input when restoring a reference frame at time t , I_t^{LQ} , and denote them as $[I_{t-N}^{LQ}, \dots, I_{t+N}^{LQ}]$. This process is repeated for every consecutive sequence of $2N + 1$ frames using shifted window approach. As illustrated in Figure 2, the proposed network can be primarily divided into two parts: (1) temporal context extraction, (2) joint flow and feature refinement module, which is trained on temporal loss with occlusion-aware masking.

3.2. Integrating Temporal Context

The 3D convolutions are applied to the consecutive input frames to exploit the temporal context. For a consecutive sequence of $2N + 1$ frames, we represent extracted spatio-

temporal features as $F^i \in \mathbb{R}^{(2N+1) \times H' \times W' \times C'}$, where H' , W' are the spatial dimensions and C' is the number of output channels. In addition, temporal information between input frames is further exploited by explicit motion modeling through optical flow. To be more specific, the optical flow is computed using the pre-trained RAFT [39] model on $2N$ LQ frames with respect to the current frame, I_t^{LQ} . The initial optical flow between I_t^{LQ} and I_{t-N}^{LQ} is denoted as $\Delta_{t,t-N}^0$. The temporally rich features obtained through 3D convolutions together with optical flow information are then passed to joint flow and feature refinement module.

3.3. Joint Flow and Feature Refinement Module

The initial optical flow is computed on LQ frames, its accuracy can be affected due to the presence of degradation in the input frames. The proposed JFFR module is focused on jointly correcting the initial flow and then refining frame features in an alternating manner.

Without any loss in generality, the proposed method is described with a sequence of 3 consecutive frames (*i.e.*, $N = 3$). Initially, the spatio-temporal features (*i.e.*, the input frames) $F^0 = [F_{t-1}^0, F_t^0, F_{t+1}^0]$ and flow (*i.e.*, optical flow on input frames) $[\Delta_{t,t-1}^0, \Delta_{t,t+1}^0]$ are passed as input to the JFFR module. Specifically, given an input features and associated flow to the i -th level of encoder or decoder, the refined flow and features can be formulated as,

$$F^{i+1}, \Delta_{t,t-1}^{i+1}, \Delta_{t,t+1}^{i+1} = \text{JFFR}(F^i, \Delta_{t,t-1}^i, \Delta_{t,t+1}^i). \quad (1)$$

The proposed JFFR module first corrects the initial flow using cost volume and then refine frame features using the corrected flow in an alternating manner.

3.3.1. Cost volume computation

The cost volume is computed independently on previous and next frame with respect to the reference frame. For the sake of simplicity, we present the cost volume computation with respect to previous frame only. The cost volume is computed in two steps. First, the features F_{t-1}^i are spatially transformed using the corresponding flow $\Delta_{t,t-1}^i$. It can be represented as,

$$F_{t-1}^{i,Proj} = \mathcal{T}(F_{t-1}^i, \Delta_{t,t-1}^i), \quad (2)$$

where $\mathcal{T}(\cdot)$ is a function that projects or spatially transform the features using corresponding flow values. We use grid sampling to transform the features using flow values.

The cost volume is constructed to capture the L_1 distance between the features of the current frame and projected frame over a 9×9 search window. It is represented mathematically as,

$$C = \mathcal{F}(F_{t-1}^{i,Proj}, F_t^i) \in \mathbb{R}^{d_h \times d_w \times H' \times W'}, \quad (3)$$

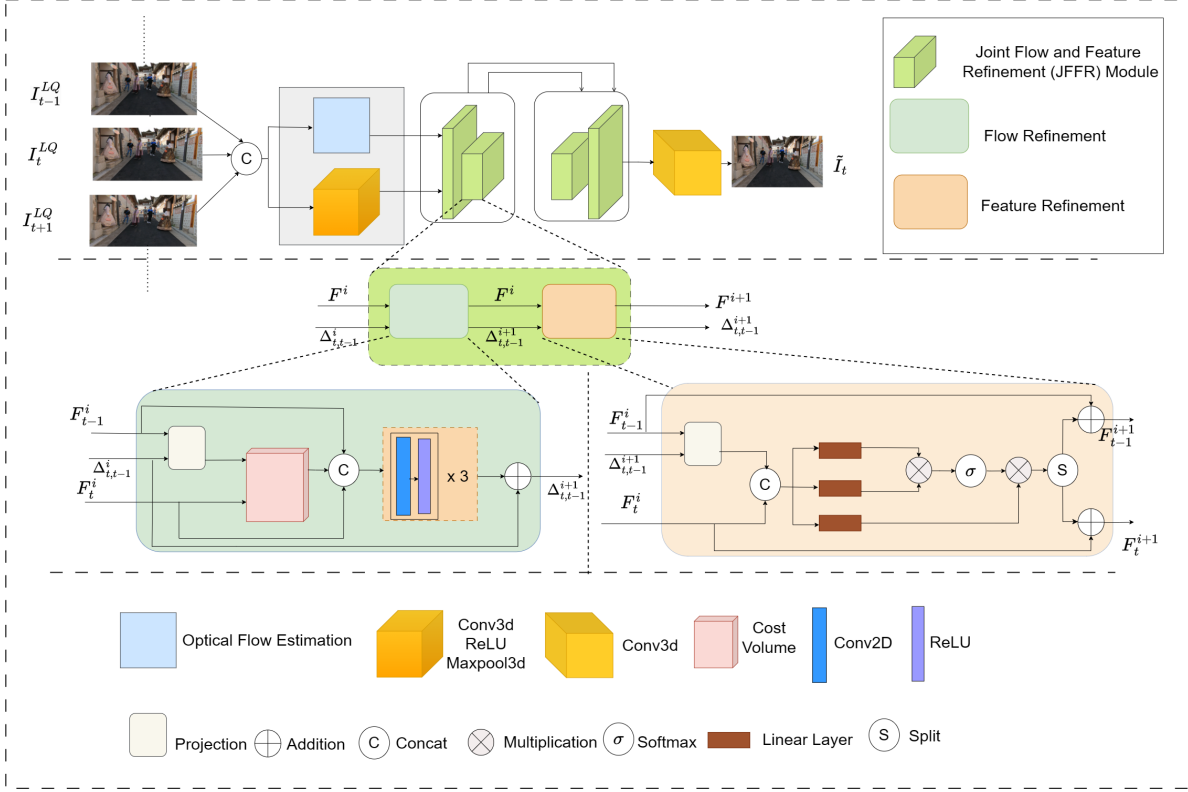


Figure 2. Architecture of the proposed joint flow and feature refinement using attention framework(JFFRA).

where $\mathcal{F}(\cdot)$ is a function that transform 3D features into 4D cost volume. Here, d_h and d_w are the search dimensions in x and y directions, such that,

$$\mathcal{C}[l, m, h, w] = \left\| F_t^i[h, w] - F_{t-1}^{i, Proj}[h + l, w + m] \right\|_1, \quad (4)$$

where $l, m \in [-4, 4]$ based on the size of search window 9×9 .

The cost volume reflects the correlation between features of the current frame and associated features inside the search window of the projected frame. In order to produce the final result, we still need to decide maximum similarity matching within the search window for each feature of the reference frame. Therefore, the computed cost volume \mathcal{C} in conjunction with feature maps are processed using flow head network. The flow head refines flow values by utilizing the similarity information encoded in the cost volume. To ease the burden of feature learning, we employ offset flow learning and only predict deviation from the previously computed flow. The updated flow is given as,

$$\Delta_{t,t-1}^{i+1} = \Delta_{t,t-1}^i + \text{Flow Head}(\mathcal{C}, F_t^i, F_{t-1}^i). \quad (5)$$

3.3.2. Feature refinement

In this section, we integrate attention mechanism to refine features using the updated flow. Given a previous and next

frame features F_{t-1}^i and F_{t+1}^i respectively, the updated features are computed as:

$$F_{t-1}^{i, Update} = \mathcal{T}(F_{t-1}^i, \Delta_{t,t-1}^{i+1}), \quad (6)$$

$$F_{t+1}^{i, Update} = \mathcal{T}(F_{t+1}^i, \Delta_{t,t+1}^{i+1}). \quad (7)$$

We then concatenate updated and reference frame features and compute the *query* Q^i , *key* K^i and *value* V^i by linear projection as:

$$F_t^{i, Con} = F_t^i \textcircled{C} F_{t-1}^{i, Update} \textcircled{C} F_{t+1}^{i, Update}, \quad (8)$$

$$Q_t^i = F_t^{i, Con} W^Q, \quad K_t^i = F_t^{i, Con} W^K, \quad V_t^i = F_t^{i, Con} W^V, \quad (9)$$

where the operator \textcircled{C} represents concatenation and W^Q , W^K and W^V are learned projection matrices. We then compute attention map, A_t^i , using *query* and *key*. Finally, residuals are extracted as:

$$\mathcal{R}_t^i, \mathcal{R}_{t-1}^i, \mathcal{R}_{t+1}^i = A_t^i V_t^i. \quad (10)$$

The refined feature maps are computed as:

$$F_t^{i+1}, F_{t-1}^{i+1}, F_{t+1}^{i+1} = F_t^i + \mathcal{R}_t^i, F_{t-1}^i + \mathcal{R}_{t-1}^i, F_{t+1}^i + \mathcal{R}_{t+1}^i. \quad (11)$$

We propagate the refined flow and features along to next level as shown in Figure 2.

3.4. Temporal Consistency Loss with Occlusion-Aware Masking

One of the most important challenges in video restoration is to reduce flickering. The flickering causes unnatural temporal fluctuations in perceived video, thereby creating an annoying artifact. Hence, maintaining temporal consistency between successive frames is the stringent requirement in video restoration. While current SOTA methods rely intrinsically on motion modeling to compensate flickering, this problem is overlooked in the existing literature.

In this section, a temporal loss is proposed to deliberately eliminate flickering. It is important to note that flickering artifacts are severely observed in regions of the video that are nearly still (i.e. there is no or small motion across frames). For that reason, the proposed loss leverages on optical flow and occlusion-aware mask to align restored frames effectively. This loss computes the difference between reconstructed reference frame \tilde{I}_t and corresponding warped frame \tilde{I}_{t-1}^{warp} only for regions where there is no pixel-value variation.

The loss computation is performed in three stages. First, the optical flow $\Delta_{t,t-1}$ is computed between ground truth images I_t^{HQ} and I_{t-1}^{HQ} . It is worth noting that the optical flow is computed between clean images since loss function is used only during training. Afterwards, the restored frame \tilde{I}_{t-1} is warped towards the restored reference frame using optical flow. It can be represented as,

$$\tilde{I}_{t-1}^{warp} = \text{Warp}(\tilde{I}_{t-1}, \Delta_{t,t-1}). \quad (12)$$

In the second stage, we compute occlusion-aware mask with the ground truth frames. This mask is computed aiming to focus on regions across frames that are not occluded (i.e. regions that are visible in both frames). It is given as,

$$m_{t,t-1} = \exp(-\alpha \left\| I_t^{HQ} - I_{t-1}^{HQ,warp} \right\|_2^2), \quad (13)$$

where $I_{t-1}^{HQ,warp} = \text{Warp}(I_{t-1}^{HQ}, \Delta_{t,t-1})$. Here, the parameter α should be sufficiently large to allow fast transition from 1 to 0 and efficiently penalize the large and non-zero frame differences.

In the last stage, we compute the distance between \tilde{I}_t and \tilde{I}_{t-1}^{warp} . Then we apply mask on the computed distance, thus obtaining loss value for non-occluded regions:

$$\mathcal{L}_{t,t-1}^T = m_{t,t-1} \odot \left\| \tilde{I}_t - \tilde{I}_{t-1}^{warp} \right\|_1, \quad (14)$$

where operator \odot performs element-wise multiplication.

3.5. Total Loss

The total loss is combination of the temporal consistency loss and well-known L_1 distance (absolute error) between reconstructed and ground-truth frame.

$$\mathcal{L}_{Total} = \left\| I_t^{HQ} - \tilde{I}_t \right\|_1 + w_1 \cdot \mathcal{L}_{t,t-1}^T + w_2 \cdot \mathcal{L}_{t,t+1}^T, \quad (15)$$

where w_1 and w_2 are weighting factors that balance the trade-off between L_1 loss and temporal consistency loss. We set w_1 and w_2 to 0.2 in our experiments. Refer to supplementary material for visual results that demonstrate the significance of this loss function in reducing flickering artifacts.

4. Experiments

In this section, we report a detailed experimental analysis to test the effectiveness of the proposed JFFRA framework on various video restoration tasks. The ablation studies are carried out to signify the contribution of each component of the proposed framework. The performance analysis of the proposed method in comparison with SOTA methods is presented for video denoising, video delblurring and video super-resolution tasks. The performance is evaluated in terms of PSNR and SSIM.

4.1. Experimental Setup

For all experiments, the stack of 3 consecutive frames is used as the input. Attention is computed on a window size of 8. The network is trained using the Adam optimizer for 700k iterations. The learning rate of the optimizer is set to $1e - 4$ which decreases to $1e - 6$ using step learning rate scheduler. The network is trained with mini-batches of size 48 and hyper-parameter α is set to 0.2. All experiments are performed on 8 Tesla P40 cards with 24 GB of memory.

4.2. Video Denoising

4.2.1 Real Denoising Dataset: The CRVD dataset [57] is captured in raw domain and converted to sRGB domain using image signal processing module. The dataset contains 6 indoor scenes for training and 5 indoor scenes for testing. For each scene, the dataset has 5 different ISO settings ranging from 1600 to 25600. In Table 1, performance of the proposed method on CRVD dataset under different ISO settings is presented. It can be seen that the proposed method achieves best metrics across all ISO settings. The most encouraging finding is that the proposed method beats previous SOTA method by 1.62 dB in PSNR. This improvement in the performance can be attributed to JFFR module for jointly refining the flow and features, thereby efficiently handling temporal information.

Table 1. Quantitative analysis of the proposed JFFRA network with SOTA methods for video denoising on the CRVD (RGB) datasets [57]. The best and second best results are highlighted in red and blue colors, respectively.

Metrics	VBM4D [24] TIP' 12	ViDeNN [10] CVPR' 19	TOFlow [51] IJCV' 19	SMD [9] ICCV' 19	EDVR [45] CVPR' 19	DIDN [54] CVPR' 19	RViDeNet [57] CVPR' 20	Ours
PSNR	34.16	31.48	34.81	35.87	38.97	38.83	39.95	41.57
SSIM	0.922	0.826	0.921	0.957	0.972	0.974	0.979	0.986

Table 2. Quantitative analysis with different existing methods for video denoising on the DAVIS [16] and Set-8 [37] datasets. The parameter σ indicates the noise level. The best and second best results are highlighted in red and blue colors, respectively.

Datasets	σ	VBM4D [24] TIP' 12	VNLB [2] JMJC' 18	DVDnet [37] ICIP' 19	FastDVDnet [38] CVPR' 20	VNLNet [11] ICIP' 2019	PaCNet [42] ICCV' 21	BasicVSR++ [7] CVPR' 19	R-VRT [22] NeurIPS' 22	Tempformer [32] ECCV' 22	ShiftNet [20] CVPR' 23	VRT [23] TIP' 24	Ours
DAVIS [16]	10	37.58/-	38.85/-	38.13/9657	38.71/9672	39.56/9707	39.97/9713	40.13/9754	40.57/-	40.17/-	40.91/-	40.82/9776	41.13/9781
	20	33.88/-	35.68/-	35.70/9422	35.77/9405	36.53/9464	37.10/9470	37.41/9598	38.05/-	37.36/-	38.34/-	38.15/9625	38.54/9652
	30	31.65/-	33.73/-	34.08/9188	34.04/9167	-/-	35.07/9211	35.74/9456	36.57/-	35.66/-	36.83/-	36.52/9483	37.04/9569
	40	30.05/-	32.32/-	32.86/8962	32.82/8949	33.32/8996	33.57/8969	34.49/9319	35.47/-	34.42/-	35.71/-	35.32/9345	35.67/9362
	50	28.80/-	31.13/-	31.85/8745	31.86/8747	-/-	32.39/8743	33.45/9179	34.57/-	33.44/-	34.82/-	34.36/9211	34.65/9321
Set-8 [37]	10	36.05/-	37.26/-	36.08/9510	36.44/9540	37.28/9606	37.06/9590	36.83/9574	37.53/-	37.15/-	37.48/-	37.88/9630	38.17/9642
	20	32.18/-	33.72/-	33.49/9182	33.43/9196	34.02/9273	33.94/9247	34.15/9319	34.83/-	34.74/-	34.85/-	35.02/9373	35.22/9386
	30	30.00/-	31.74/-	31.68/8862	31.68/8889	-/-	32.05/8921	32.57/9095	33.30/-	33.20/-	33.29/-	33.35/9141	33.30/9118
	40	28.48/-	30.39/-	30.46/8564	30.46/8608	30.72/8622	30.70/8623	30.42/8589	32.21/-	32.06/-	32.18/-	32.15/8928	32.06/8842
	50	27.33/-	29.24/-	29.53/8289	29.53/8351	-/-	29.66/8349	30.49/8690	31.33/-	31.16/-	31.33/-	31.22/8733	31.24/8726

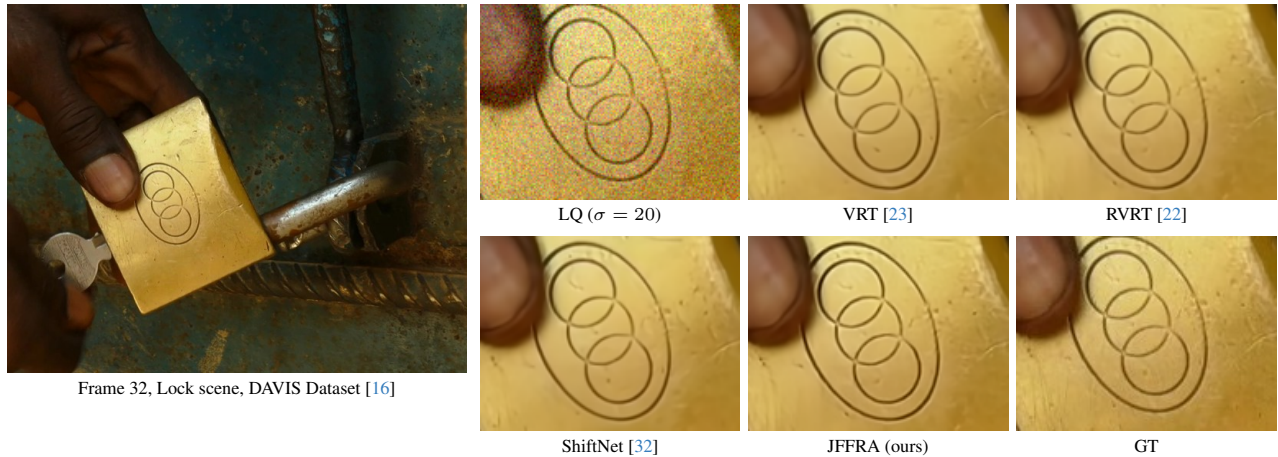


Figure 3. Visual comparison on video denoising task. The JFFRA effectively remove noise while preserving structure and sharpness.

4.2.2 Synthetic Video Denoising : DAVIS [16] and Set-8 [37] are the standard synthetic video denoising datasets. While DAVIS consists of 90 training and 30 testing sequences, Set-8 have 8 testing video sequences. Following the synthetic pipeline setting as VRT [23], noisy sequences are synthesized by adding AWGN with noise level $\sigma \in [0,50]$ on the DAVIS training set.

The evaluation is performed on Davis and Set-8 test data with noise levels $\sigma = \{10, 20, 30, 40, 50\}$. It can be observed from Table 2 that JFFRA outperforms existing methods on DAVIS dataset while giving competitive performance on Set-8 dataset. Additionally, it can be visualized from Figure 3 that the proposed method denoises video frames while maintaining the texture and high frequency regions compared to other methods.

4.3. Video Super Resolution

The comparative analysis of various methods on video super-resolution ($\times 4$) task is detailed in Table 3. The

network is trained with both bi-cubic (BI) and blur-down sampling (BD) degradations on standard datasets such as REDS (RGB) [26] and Vimeo-90K [52]. The performance is evaluated our Vimeo-90k, REDS, Vid4 [2], and UDM10 [53] dataset. It can be noticed that the proposed method achieves the best performance on both BI and BD degradations. While JFFRA outperforms SOTA VRT [23] by 0.26 \sim 0.6 dB on REDS and Vid4 dataset, it surpasses VRT by 1 \sim 1.3 dB on Vimeo-90K and UDM10 dataset. This performance improvement signifies that the proposed offset flow learning and residual feature refinement guides the network to converge to a better optimal minimum. The qualitative results are displayed in Figure 4 for visual analysis. It can be noticed that the proposed method is able to retain texture more precisely and robust to detail loss as compared to other methods.

Table 3. Quantitative analysis of different methods in terms of PSNR/SSIM for video super-resolution ($\times 4$) using BI and BD degradation settings on various datasets. The best and second best results are highlighted in red and blue colors, respectively.

Method	Publication	Training Frames (REDS/Vimeo-90K)	BI Degradation			BD Degradation		
			REDS4 (RGB) [26]	Vimeo-90K-T (Y) [52]	Vid4 (Y) [2]	UDM10 (Y) [53]	Vimeo-90K-T (Y) [52]	Vid4 (Y) [2]
Bicubic	-	-	26.14/0.7292	31.32/0.8684	23.78/0.6347	28.47/0.8253	31.30/0.8687	21.80/0.5246
SwinIR [21]	ICCV'21	-	29.05/0.8269	35.67/0.9287	25.68/0.7491	35.42/0.9380	34.12/0.9167	25.25/0.7262
TOFlow [51]	IJCV'19	5/7	27.98/0.7990	33.08/0.9054	25.89/0.7651	36.26/0.9438	34.62/0.9212	25.85/0.7659
DUF [15]	CVPR'18	7/7	28.63/0.8251	-	27.33/0.8319	38.48/0.9605	36.87/0.9447	27.38/0.8329
PFNL [53]	ICCV'19	7/7	29.63/0.8502	36.14/0.9363	26.73/0.8029	38.74/0.9627	-	27.16/0.8355
RBPN [13]	CVPR'19	7/7	30.09/0.8590	37.07/0.9435	27.12/0.8180	38.66/0.9596	37.20/0.9458	27.17/0.8205
EDVR [45]	CVPR'19	5/7	31.09/0.8800	37.61/0.9489	27.35/0.8264	39.89/0.9686	37.81/0.9523	27.85/0.8503
BasicVSR [7]	CVPR'21	15/14	31.42/0.8909	37.18/0.9450	27.24/0.8251	39.96/0.9694	37.53/0.9498	27.96/0.8553
IconVSR [7]	CVPR'21	15/14	31.67/0.8948	37.47/0.9476	27.39/0.8279	40.03/0.9694	37.84/0.9524	28.04/0.8570
BasicVSR++ [8]	CVPR'22	30/14	32.39/0.9069	37.79/0.9500	27.79/0.8400	40.72/0.9722	38.21/0.9550	29.04/0.8753
RVRT [22]	NeurIPS'22	16/7	32.75/0.9113	38.15/0.9527	27.99/0.8462	40.90/0.9729	38.59/0.9576	29.54/0.8810
VRT [23]	TIP'24	16/7	32.19/0.9006	38.20/0.9530	27.9/0.8425	41.05/0.9737	38.72/0.9584	29.42/0.8795
JFFRA (ours)	-	3/3	32.45/0.9136	39.32/0.9561	28.54/0.8725	42.15/0.9848	39.62/0.9786	30.52/0.8896

Table 4. Quantitative analysis of various methods in terms of PSNR/SSIM for video deblurring on DVD [34]. The best and second best results are highlighted in red and blue colors, respectively.

Metric	DBN [34]	DBLRNet [59]	STFAN [61]	STTN [18]	SFE [50]	EDVR [45]	TSP [28]	PVDNet [31]	GSTA [35]	ARVo [19]	R-VRT [22]	VRT [23]	ShiftNet [20]	BSSTNet [58]	Ours
PSNR	30.01	30.08	31.24	31.61	31.71	31.82	32.13	32.31	32.53	32.80	34.30	34.27	34.69	34.95	35.15
SSIM	0.8877	0.8845	0.9340	0.9160	0.9160	0.9160	0.9268	0.9260	0.9468	0.9352	0.9655	0.9651	0.969	0.97	0.976

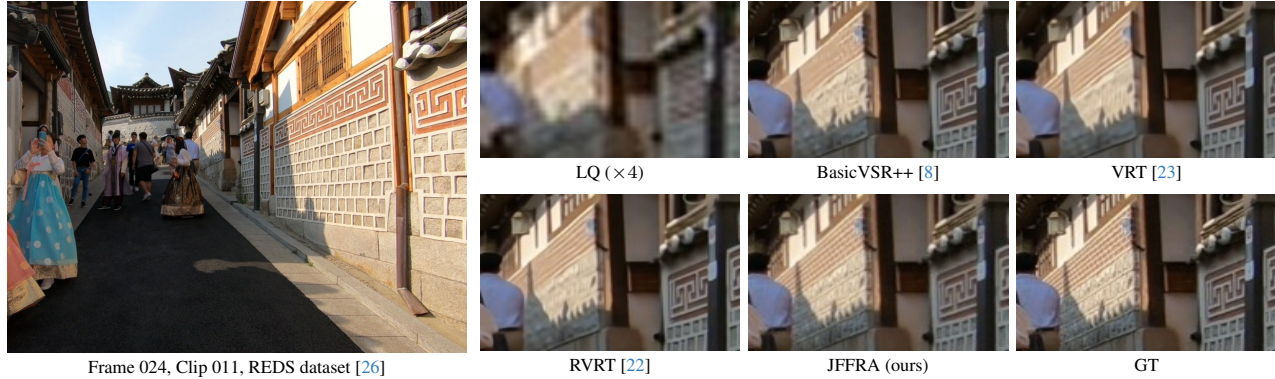


Figure 4. Visual comparison on video super-resolution ($\times 4$) task. The proposed JFFRA recovers wall structure and fine patterns efficiently.

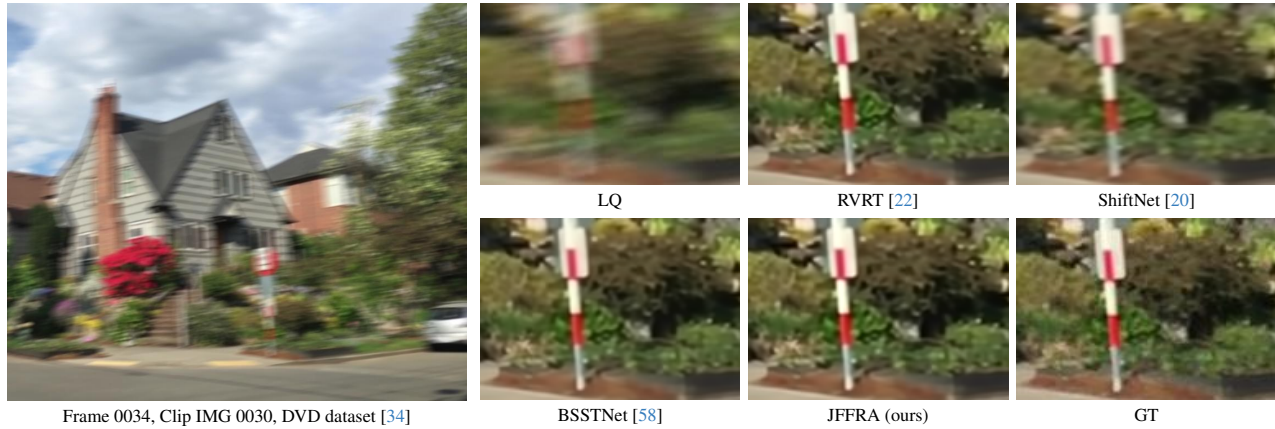


Figure 5. Visual comparison on video deblurring task. The restored image using JFFRA is more sharper and closer to ground truth.

4.4. Video Deblurring

The usefulness of the proposed method in practical applications is demonstrated by performing experiments on video deblurring task. The experiments are conducted on the DVD [34] dataset. It is clear from the results shown in Table 4 that the proposed method yields promising results

and attains SOTA performance. The proposed method surpasses ShiftNet [20] and BSSTNet [58] by 0.46 dB and 0.2 dB respectively. Figure 5 shows the visual comparison between various methods. It can be visualized that the proposed method effectively removes the blur while restoring the fine details. This observation is consistent with the im-

proved quantitative performance.

4.5. Computational Cost

Figure 6 shows that our method achieves the optimal trade-off between computational cost and restoration performance. The complexity of JFFRA is much lower than VRT [23], ShiftNet [20] while achieving much better performance. Refer supplementary for detailed analysis.

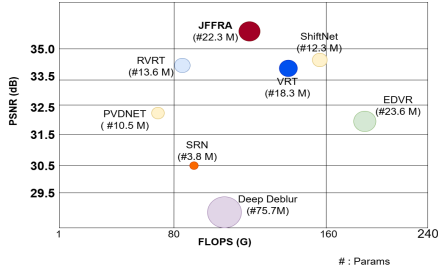


Figure 6. Complexity Analysis of JFFRA with other state-of-the-art networks on Video Deblurring Task.

5. Ablation Studies

We conducted several experiments to demonstrate the effectiveness of the proposed JFFR block and temporal loss function.

Impact of JFFR Module : We replace the proposed block with four variations: 1) Mutual self-attention substituting without parallel warping similar to [23], 2) attention with learnable offsets, 3) attention without refined flow, and 4) attention with iterative refined flow. The quantitative results on the DVD deblur dataset as detailed in Table 5, reveal that joint refinement of flow and feature in iterative manner complement each other, thereby significantly improving the performance.

Table 5. Ablation results on proposed JFFR Module.

Methods	PSNR	SSIM
Temporal mutual self attention	28.5	0.87
Attention with learnable offset	28.72	0.884
Attention without refined flow	29.45	0.897
JFFR	35.15	0.976

Impact of Flow Refinement Module : Many researchers have explored the use of optical flow for video restoration tasks. In all the previous works, flow is computed either on degraded input or initial recovered frames, without continuous refinement. To demonstrate the effectiveness of iterative flow refinement, we initially trained our network without flow refinement module. It can be clearly seen from Table 5 that lack of flow refinement causes heavy losses in the restoration. This poor recovery performance can be attributed to fundamental flaws in the initial flow.

We further showcase in Figure 7 the impact of flow refinement. It can be deduced from Table 5 and Figure 7 that joint refinement of frame features and flow together with their complementary enhancement fuels persistent improvement.

Impact of Temporal Loss Function : The importance of temporal loss function in reducing flickering artifacts is summarized in Table 6. The temporal consistency between successive frames is measured using the optical flow based warping metric (OPW) following FMNet [49] and DPT [47]. The efficiency of the proposed temporal loss function in reducing inconsistency between successive frames can be concluded from Table 6. Refer to supplementary material for more detailed and visual analysis.

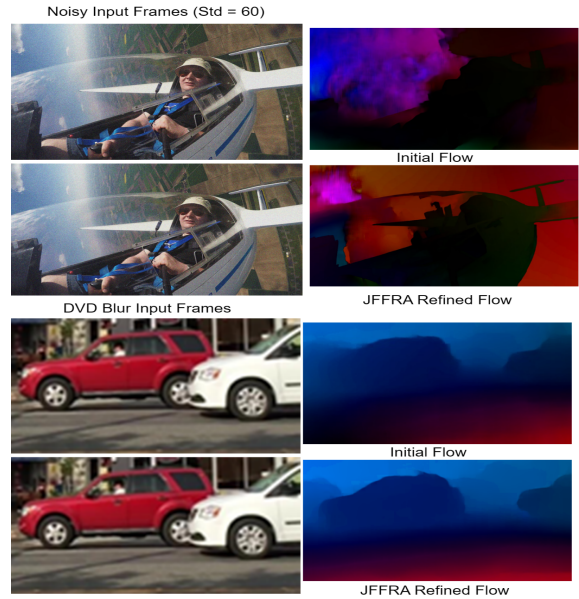


Figure 7. Impact of flow refinement in retrieving the information from low quality frames. Frames used are Davis-Test [16] (aerobatics frame 13, 14) and DVD [34] (IMG0037, frame 13,14)

Table 6. Ablation results to show usefulness of the proposed temporal loss function.

Methods	OPW
JFFRA without temporal loss	0.372
JFFRA with temporal loss	0.354

6. Conclusions

In this paper, we propose a novel joint flow and feature refinement using attention framework for video restoration. Unlike previous end-to-end learning approaches, JFFRA utilizes an iterative refinement process that builds on collaborative synergy between flow and restoration. At each stage, the flow refinement module refines the current flow field based on existing enhanced features information, while the feature refinement block uses the refined flow to further

enhance feature alignment and information fusion. Through this mutual collaboration, JFFRA effectively addresses the limitations of traditional methods. Comprehensive experiments on various restoration tasks and benchmark datasets validate the versatility and superiority of JFFRA, establishing its position as a leading solution in the field. With up to 1.62 dB gain in PSNR compared to state-of-the-art methods, JFFRA sets a new standard for video restoration algorithms.

References

- [1] Dawit Mureja Argaw, Junsik Kim, Francois Rameau, Chaoning Zhang, and In So Kweon. Restoration of video frames from a single blurred image with motion understanding. In *Proceedings of the IEEE/CVF Conference on Computer Vision and Pattern Recognition*, pages 701–710, 2021. 1
- [2] Pablo Arias and Jean-Michel Morel. Video denoising via empirical bayesian estimation of space-time patches. *Journal of Mathematical Imaging and Vision*, 60:70–93, 2018. 6, 7
- [3] Antoni Buades, Jose-Luis Lisani, and Marko Miladinović. Patch-based video denoising with optical flow estimation. *IEEE Transactions on Image Processing*, 25(6):2573–2586, 2016. 2
- [4] Jose Caballero, Christian Ledig, Andrew Aitken, Alejandro Acosta, Johannes Totz, Zehan Wang, and Wenzhe Shi. Real-time video super-resolution with spatio-temporal networks and motion compensation. In *Proceedings of the IEEE conference on computer vision and pattern recognition*, pages 4778–4787, 2017. 2
- [5] Jiezhong Cao, Yawei Li, Kai Zhang, and Luc Van Gool. Video super-resolution transformer. *arXiv*, 2021. 2
- [6] Jiezhong Cao, Jingyun Liang, Kai Zhang, Yawei Li, Yulun Zhang, Wenguan Wang, and Luc Van Gool. Reference-based image super-resolution with deformable attention transformer. In *European conference on computer vision*, 2022. 2
- [7] Kelvin CK Chan, Xintao Wang, Ke Yu, Chao Dong, and Chen Change Loy. Basicvnr: The search for essential components in video super-resolution and beyond. In *Proceedings of the IEEE/CVF conference on computer vision and pattern recognition*, pages 4947–4956, 2021. 6, 7
- [8] Kelvin CK Chan, Shangchen Zhou, Xiangyu Xu, and Chen Change Loy. Basicvnr++: Improving video super-resolution with enhanced propagation and alignment. In *IEEE Conference on Computer Vision and Pattern Recognition*, 2022. 3, 7
- [9] Chen Chen, Qifeng Chen, Minh N Do, and Vladlen Koltun. Seeing motion in the dark. In *IEEE International Conference on Computer Vision*, pages 3185–3194, 2019. 6
- [10] Michele Claus and Jan van Gemert. Videnn: Deep blind video denoising. In *IEEE Conference on Computer Vision and Pattern Recognition Workshops*, 2019. 3, 6
- [11] Axel Davy, Thibaud Ehret, Jean-Michel Morel, Pablo Arias, and Gabriele Facciolo. Non-local video denoising by cnn. *arXiv preprint arXiv:1811.12758*, 2018. 6
- [12] Philipp Fischer, Alexey Dosovitskiy, Eddy Ilg, Philip Häusser, Caner Hazırbaş, Vladimir Golkov, Patrick Van der Smagt, Daniel Cremers, and Thomas Brox. Flownet: Learning optical flow with convolutional networks. *arXiv preprint arXiv:1504.06852*, 2015. 2, 3
- [13] Muhammad Haris, Gregory Shakhnarovich, and Norimichi Ukita. Recurrent back-projection network for video super-resolution. In *Proceedings of the IEEE/CVF conference on computer vision and pattern recognition*, pages 3897–3906, 2019. 7
- [14] Yan Huang, Wei Wang, and Liang Wang. Bidirectional recurrent convolutional networks for multi-frame super-resolution. *Advances in neural information processing systems*, 28, 2015. 2
- [15] Younghyun Jo, Seoung Wug Oh, Jaeyeon Kang, and Seon Joo Kim. Deep video super-resolution network using dynamic upsampling filters without explicit motion compensation. In *Proceedings of the IEEE conference on computer vision and pattern recognition*, pages 3224–3232, 2018. 7
- [16] Anna Khoreva, Anna Rohrbach, and Bernt Schiele. Video object segmentation with language referring expressions. In *Computer Vision—ACCV 2018: 14th Asian Conference on Computer Vision, Perth, Australia, December 2–6, 2018, Revised Selected Papers, Part IV 14*, pages 123–141. Springer, 2019. 6, 8
- [17] Taewoo Kim, Jaeseok Jeong, Hoonhee Cho, Yuhwan Jeong, and Kuk-Jin Yoon. Towards real-world event-guided low-light video enhancement and deblurring. *arXiv preprint arXiv:2408.14916*, 2024. 1, 2
- [18] Tae Hyun Kim, Mehdi SM Sajjadi, Michael Hirsch, and Bernhard Scholkopf. Spatio-temporal transformer network for video restoration. In *Proceedings of the European conference on computer vision (ECCV)*, pages 106–122, 2018. 7
- [19] Dongxu Li, Chenchen Xu, Kaihao Zhang, Xin Yu, Yiran Zhong, Wenqi Ren, Hanna Suominen, and Hongdong Li. Arvo: Learning all-range volumetric correspondence for video deblurring. In *Proceedings of the IEEE/CVF Conference on Computer Vision and Pattern Recognition*, pages 7721–7731, 2021. 1, 2, 7
- [20] Dasong Li, Xiaoyu Shi, Yi Zhang, Ka Chun Cheung, Simon See, Xiaogang Wang, Hongwei Qin, and Hongsheng Li. A simple baseline for video restoration with grouped spatial-temporal shift. In *Proceedings of the IEEE/CVF Conference on Computer Vision and Pattern Recognition*, pages 9822–9832, 2023. 6, 7, 8
- [21] Jingyun Liang, Jiezhong Cao, Guolei Sun, Kai Zhang, Luc Van Gool, and Radu Timofte. Swinir: Image restoration using swin transformer. In *Proceedings of the IEEE/CVF international conference on computer vision*, pages 1833–1844, 2021. 1, 7
- [22] Jingyun Liang, Yuchen Fan, Xiaoyu Xiang, Rakesh Ranjan, Eddy Ilg, Simon Green, Jiezhong Cao, Kai Zhang, Radu Timofte, and Luc V Gool. Recurrent video restoration transformer with guided deformable attention. *Advances in Neural Information Processing Systems*, 35:378–393, 2022. 1, 2, 6, 7

- [23] Jingyun Liang, Jiezhong Cao, Yuchen Fan, Kai Zhang, Rakesh Ranjan, Yawei Li, Radu Timofte, and Luc Van Gool. Vrt: A video restoration transformer. *IEEE Transactions on Image Processing*, 2024. 1, 2, 3, 6, 7, 8
- [24] Matteo Maggioni, Giacomo Boracchi, Alessandro Foi, and Karen Egiazarian. Video denoising, deblurring, and enhancement through separable 4-d nonlocal spatiotemporal transforms. *IEEE Transactions on Image Processing*, 2012. 6
- [25] Matteo Maggioni, Yibin Huang, Cheng Li, Shuai Xiao, Zhongqian Fu, and Fenglong Song. Efficient multi-stage video denoising with recurrent spatio-temporal fusion. In *IEEE Conference on Computer Vision and Pattern Recognition*, 2021. 2, 3
- [26] Seungjun Nah, Tae Hyun Kim, and Kyoung Mu Lee. Deep multi-scale convolutional neural network for dynamic scene deblurring, 2018. 6, 7
- [27] Seungjun Nah, Sungyong Baik, Seokil Hong, Gyeongsik Moon, Sanghyun Son, Radu Timofte, and Kyoung Mu Lee. Ntire 2019 challenge on video deblurring and super-resolution: Dataset and study. In *Proceedings of the IEEE/CVF conference on computer vision and pattern recognition workshops*, pages 0–0, 2019. 1
- [28] Jinshan Pan, Haoran Bai, and Jinhui Tang. Cascaded deep video deblurring using temporal sharpness prior. In *Proceedings of the IEEE/CVF conference on computer vision and pattern recognition*, pages 3043–3051, 2020. 7
- [29] Zhihang Ren, Jijia Li, Shuaicheng Liu, and Bing Zeng. Meshflow video denoising. In *2017 IEEE International Conference on Image Processing (ICIP)*, pages 2966–2970, 2017. 2
- [30] Dev Yashpal Sheth, Sreyas Mohan, Joshua L Vincent, Ramon Manzorro, Peter A Crozier, Mitesh M Khapra, Eero P Simoncelli, and Carlos Fernandez-Granda. Unsupervised deep video denoising. In *Proceedings of the IEEE/CVF international conference on computer vision*, pages 1759–1768, 2021. 1
- [31] Hyeonseok Son, Junyong Lee, Jonghyeop Lee, Sunghyun Cho, and Seungyong Lee. Recurrent video deblurring with blur-invariant motion estimation and pixel volumes. *ACM Transactions on Graphics (TOG)*, 40(5):1–18, 2021. 7
- [32] Mingyang Song, Yang Zhang, and Tunç O Aydın. Tempformer: Temporally consistent transformer for video denoising. In *European conference on computer vision*, pages 481–496. Springer, 2022. 6
- [33] Ralf C Staudemeyer and Eric Rothstein Morris. Understanding lstm—a tutorial into long short-term memory recurrent neural networks. *arXiv preprint arXiv:1909.09586*, 2019. 2
- [34] Shuochen Su, Mauricio Delbracio, Jue Wang, Guillermo Sapiro, Wolfgang Heidrich, and Oliver Wang. Deep video deblurring for hand-held cameras. In *Proceedings of the IEEE conference on computer vision and pattern recognition*, pages 1279–1288, 2017. 2, 7, 8
- [35] Maitreya Suin and AN Rajagopalan. Gated spatio-temporal attention-guided video deblurring. In *Proceedings of the IEEE/CVF Conference on Computer Vision and Pattern Recognition*, pages 7802–7811, 2021. 7
- [36] Deqing Sun, Xiaodong Yang, Ming-Yu Liu, and Jan Kautz. Pwc-net: Cnns for optical flow using pyramid, warping, and cost volume. In *Proceedings of the IEEE conference on computer vision and pattern recognition*, pages 8934–8943, 2018. 2
- [37] Matias Tassano, Julie Delon, and Thomas Veit. Dvdnet: A fast network for deep video denoising. In *IEEE International Conference on Image Processing*, 2019. 2, 3, 6
- [38] Matias Tassano, Julie Delon, and Thomas Veit. Fastdvdnet: Towards real-time deep video denoising without flow estimation. In *IEEE Conference on Computer Vision and Pattern Recognition*, 2020. 3, 6
- [39] Zachary Teed and Jia Deng. Raft: Recurrent all-pairs field transforms for optical flow. In *Computer Vision—ECCV 2020: 16th European Conference, Glasgow, UK, August 23–28, 2020, Proceedings, Part II 16*, pages 402–419. Springer, 2020. 2, 3
- [40] Yapeng Tian, Yulun Zhang, Yun Fu, and Chenliang Xu. Tdan: Temporally-deformable alignment network for video super-resolution. In *Proceedings of the IEEE/CVF conference on computer vision and pattern recognition*, pages 3360–3369, 2020. 2
- [41] Quang-Trung Truong, Duc Thanh Nguyen, Binh-Son Hua, and Sai-Kit Yeung. Self-supervised video object segmentation with distillation learning of deformable attention. *arXiv preprint arXiv:2401.13937*, 2024. 2
- [42] Gregory Vaksman, Michael Elad, and Peyman Milanfar. Patch craft: Video denoising by deep modeling and patch matching. In *IEEE International Conference on Computer Vision*, 2021. 2, 6
- [43] Gregory Vaksman, Michael Elad, and Peyman Milanfar. Patch craft: Video denoising by deep modeling and patch matching. In *IEEE International Conference on Computer Vision*, 2021. 2
- [44] Ashish Vaswani, Noam Shazeer, Niki Parmar, Jakob Uszkoreit, Llion Jones, Aidan N Gomez, Łukasz Kaiser, and Illia Polosukhin. Attention is all you need. *Advances in neural information processing systems*, 30, 2017. 2
- [45] Xintao Wang, Kelvin CK Chan, Ke Yu, Chao Dong, and Chen Change Loy. Edvr: Video restoration with enhanced deformable convolutional networks. In *IEEE Conference on Computer Vision and Pattern Recognition Workshops*, 2019. 2, 6, 7
- [46] Yang Wang, Yi Yang, Zhenheng Yang, Liang Zhao, Peng Wang, and Wei Xu. Occlusion aware unsupervised learning of optical flow. In *Proceedings of the IEEE conference on computer vision and pattern recognition*, pages 4884–4893, 2018. 2
- [47] Yiran Wang, Min Shi, Jiaqi Li, Zihao Huang, Zhiguo Cao, Jianming Zhang, Ke Xian, and Guosheng Lin. Neural video depth stabilizer. In *Proceedings of the IEEE/CVF International Conference on Computer Vision*, pages 9466–9476, 2023. 8
- [48] Zhuofan Xia, Xuran Pan, Shiji Song, Li Erran Li, and Gao Huang. Vision transformer with deformable attention. In *Proceedings of the IEEE/CVF conference on computer vision and pattern recognition*, pages 4794–4803, 2022. 2

- [49] Ke Xian, Chunhua Shen, Zhiguo Cao, Hao Lu, Yang Xiao, Ruibo Li, and Zhenbo Luo. Monocular relative depth perception with web stereo data supervision. In *Proceedings of the IEEE Conference on Computer Vision and Pattern Recognition*, pages 311–320, 2018. [8](#)
- [50] Xinguang Xiang, Hao Wei, and Jinshan Pan. Deep video deblurring using sharpness features from exemplars. *IEEE Transactions on Image Processing*, 29:8976–8987, 2020. [7](#)
- [51] Tianfan Xue, Baian Chen, Jiajun Wu, Donglai Wei, and William T Freeman. Video enhancement with task-oriented flow. *International Journal of Computer Vision*, 127:1106–1125, 2019. [2](#), [3](#), [6](#), [7](#)
- [52] Tianfan Xue, Baian Chen, Jiajun Wu, Donglai Wei, and William T Freeman. Video enhancement with task-oriented flow. *International Journal of Computer Vision*, 127:1106–1125, 2019. [6](#), [7](#)
- [53] Peng Yi, Zhongyuan Wang, Kui Jiang, Junjun Jiang, and Jiayi Ma. Progressive fusion video super-resolution network via exploiting non-local spatio-temporal correlations. In *Proceedings of the IEEE/CVF international conference on computer vision*, pages 3106–3115, 2019. [6](#), [7](#)
- [54] Songhyun Yu, Bumjun Park, and Jechang Jeong. Deep iterative down-up cnn for image denoising. In *IEEE Conference on Computer Vision and Pattern Recognition workshops*, pages 0–0, 2019. [6](#)
- [55] Songhyun Yu, Bumjun Park, Junwoo Park, and Jechang Jeong. Joint learning of blind video denoising and optical flow estimation. In *2020 IEEE/CVF Conference on Computer Vision and Pattern Recognition Workshops (CVPRW)*, pages 2099–2108, 2020. [2](#)
- [56] Yong Yu, Xiaosheng Si, Changhua Hu, and Jianxun Zhang. A review of recurrent neural networks: Lstm cells and network architectures. *Neural computation*, 31(7):1235–1270, 2019. [2](#)
- [57] Huanjing Yue, Cong Cao, Lei Liao, Ronghe Chu, and Jingyu Yang. Supervised raw video denoising with a benchmark dataset on dynamic scenes. In *IEEE Conference on Computer Vision and Pattern Recognition*, 2020. [5](#), [6](#)
- [58] Huicong Zhang, Haozhe Xie, and Hongxun Yao. Blur-aware spatio-temporal sparse transformer for video deblurring. In *Proceedings of the IEEE/CVF Conference on Computer Vision and Pattern Recognition*, pages 2673–2681, 2024. [7](#)
- [59] Kaihao Zhang, Wenhan Luo, Yiran Zhong, Lin Ma, Wei Liu, and Hongdong Li. Adversarial spatio-temporal learning for video deblurring. *IEEE Transactions on Image Processing*, 28(1):291–301, 2018. [7](#)
- [60] Kai Zhang, Yawei Li, Jingyun Liang, Jiezhang Cao, Yulun Zhang, Hao Tang, Radu Timofte, and Luc Van Gool. Practical blind denoising via swin-conv-unet and data synthesis. *arXiv preprint arXiv:2203.13278*, 2022. [3](#)
- [61] Shangchen Zhou, Jiawei Zhang, Jinshan Pan, Haozhe Xie, Wangmeng Zuo, and Jimmy Ren. Spatio-temporal filter adaptive network for video deblurring. In *IEEE International Conference on Computer Vision*, pages 2482–2491, 2019. [7](#)
- [62] Xizhou Zhu, Han Hu, Stephen Lin, and Jifeng Dai. Deformable convnets v2: More deformable, better results. In *IEEE Conference on Computer Vision and Pattern Recognition*, 2019. [2](#)